IOP Conf. Series: Materials Science and Engineering **103** (2015) 012033 doi:10.1088/1757-899X/103/1/012033

Atomistic modeling determination of placeholder binding energy of Ti, C, and N atoms on α-Fe (100) surfaces

X J Wei, Y P Liu[1] and S P Han

College of Mechanical Engineering, Taiyuan University of Technology, Taiyuan, Shanxi, 030024, P.R. China

E-mail: lyplr@163.com

Abstract. A Fe(100) surface containing Ti, C, and N was constructed and optimized to study the placeholder binding energy of the Ti, C, and N surface atoms; this was achieved by searching the transition state with the LST (linear synchronous transit) method of the CASTEP (Cambridge Serial Total Energy Package) module. Also, the authors analyzed electron structures to determine how Ti, C, and N atoms strengthen the Fe(100) surface. The results show that when Ti, C, or N atoms take placeholder alone, or simultaneously at the Fe(100) surface, the structure stability is at its best. When including Ti, C, and N as solid solutions on the Fe(100) surface, orbital electrons of Fe3d, Ti3d, C2p, and N2p hybridize near the Fermi level; the number of electronic bonding peaks increase and bonding capacity enhances. Also, a large amount of covalent bonds formed. Covalent bonds and metallic bond coexisted.

1. Introduction

Fe is the most widely used metallic material today. As such, improving the strength and abrasion resistance of Fe-based alloy has been a popular research topic. Researchers have investigated surface modification because it can affect an alloy's abilities without affecting its strength, hardness, wear-resistance etc. Liu Y P, et al. [1-7] formed Ti and N double cementation with plasma on mild steel surfaces; the infiltration layer had an average hardness reaching 2500 HV, its corrosion resistance was 14 times better than stainless steel, its friction coefficient was 0.15, and its abrasion resistance also improved. However, the placeholder mechanism of the alloy atoms after element infiltration on the Fe surface is still unknown due to experimental conditions and a lack of supporting theories for calculation. The first-principles method is currently an effective way to solve this problem. Zhu, et al. [8] adopted the VASP (Vienna Ab-initio Simulation Package) to search the transient state, and calculated the diffusion activation energy of C in a nickel substrate. Sorescu [9] also used the same tool to calculate the diffusion activation energy and the ideal placeholder path of H in an Fe substrate, as well as on an Fe(100) surface. He believed that the activation energy of the H atoms when they diffuse from the first layer to the third layer on the Fe surface is the same as when the H atoms diffuse inside the substrate. Liu L F, et al. [10] used the LST/QST method to search the transient state among CASTEP modules, calculated the diffusion activation energy of C, N, and O in α-Fe, and determined their placeholder pathways; however, they did not consider the spin polarization of Fe. Therefore, this report will systematically study the placeholder energy of Ti, C, and N atoms in Fe substrates and on

[1] Address for correspondence:Y P Liu, College of Mechanical Engineering, Taiyuan University of Technology, Taiyuan, Shanxi, 030024, P.R. China. E-mail: lyplr@163.com.

Fe-(100) surfaces by analyzing the electron distribution; the paper also provides a theoretical explanation for why Ti, C, and N surface alloying improves Fe-based alloy.

2. Computing method

A CASTEP (Cambridge Serial Total Energy Package) module [11, 12] in Materials Studio 4.4 was used to perform the calculations. The module was based on the plane pseudo potential method under density functional theory. It replaced ionic potential with pseudo potential, and electron wave functions were expanded with plane wave basis sets. The reaction tendency between electrons was adjusted by generalized gradient approximation (GGA). All atom pseudo potential adopted ultrasoft pseudo potential, and electron wave function truncation energy was set at 300 eV. The K segmentation point of the model in the first brillouin zone was set as fine precision. The interchange correlation function was adjusted by GGA-PBE (Perdew-Burke-Ernzerhof). Before calculating property the supercell all is geometry optimization by BFGS (Broyden, Fletcher, Gold-farb, Shanno) way. Considering spin polarization and obtaining the stable structure in a local area, the admissible error was set as 1×10^{-6} eV. Moreover, at the end of the self-consistent operation process, the genetal energy converged to 1×10^{-5} eV/atom. The force at every atom was lower than 0.03 eV/nm, the tolerance excursion was less than 1×10^{-4} nm, and the stress excursion was less than 0.05 GPa.

3. Placeholder of Ti, C, N on α-Fe surface

3.1. Calculating model

Using transition metal α-Fe, whose group space is cubic system $I-m\bar{3}m$, as the subject and choosing 2.88664Å as an experimental value of the lattice parameter. In regards to the site occupancy of Ti, C and N inside the Fe-base, document [13] states that Ti atoms had slightly larger diameters than Fe atoms. Therefore, solid solution displacement occurs. The diameters of the C and N atoms are shorter; therefore, an interstitial solid solution forms, which occupies the position interstitially. When C and N undergo solid solution in octahedral interstices, there are two adjacent Fe atoms, and there will be four Fe atoms if solid solution occurs inside a tetrahedron. Since the strain energy required to move 4 atoms is greater than that required to move 2 atoms, C and N atoms take precedence in existing inside octahedral interstices.

The α-Fe(100) surface model was constructed for determining the migration of C and N atoms on the α-Fe surface, as well as Ti's effects as a placeholder. To select the appropriate surface structure layer number, the super cell structure of the Fe atom surface was constructed with 5, 6, and 7 layers. When calculating, the two outermost layers were set to be free layers; all layers below were rigid. The 10Å thick vacuum layer was established perpendicular to the lattice surface. Figure 1 shows the atomic layer used to connect the vacuum layers simulated as the actual surface.

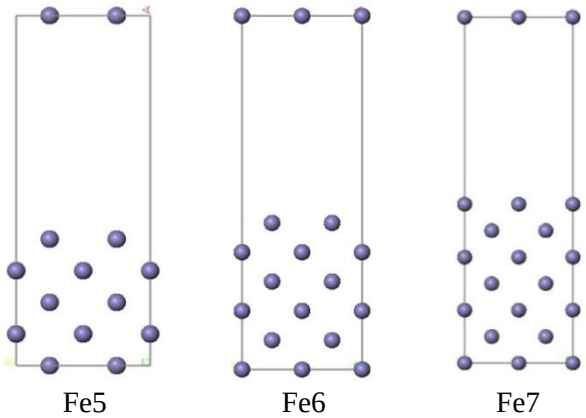

Figure 1. Fe(100) surface structure model of Fe atoms with 5, 6, and 7 atomic layers.

Geometry optimizations were performed for the Fe(100) surface structures of the Fe atoms in the 5, 6, and 7 layer models. Table 1 lists the relaxation results of atoms present in the two outermost layers; in these, Δmn=(dmn-d)/d×100% (m=1,2, n=m+1), and d is the layer interval value in the matrix unit cell. Comparing the relaxation magnitude of the three models in table 1, the sixth Fe(100) surface layer has the lowest relaxation and the calculation matched with calculations obtained by others [14, 15]; thus, the sixth Fe(100) layer was chosen to be the surface structure model to calculate the placeholder of Ti, C, and N elements on the Fe(100) surface.

Table 1. Fe(100) surface structure relaxation data of Fe atoms with 5, 6, and 7 atomic layers.

Relaxation data	Fe5	Fe6	Fe7	Others [14]
Δ_{12}(%)	-3.51	-2.67	-3.75	-2.62
Δ_{23}(%)	2.14	1.67	0.95	2.33

Figure 2 models single Ti, C, and N placeholder atoms on the Fe(100) surface; this data can be used to calculate the total energy and binding energy of the alloying surfaces with Ti, C, and N solid solution in each Fe(100) surface layer. Figure 3 shows the models of Ti atoms and C(N) atoms when they occupy positions in each Fe(100) surface layer.

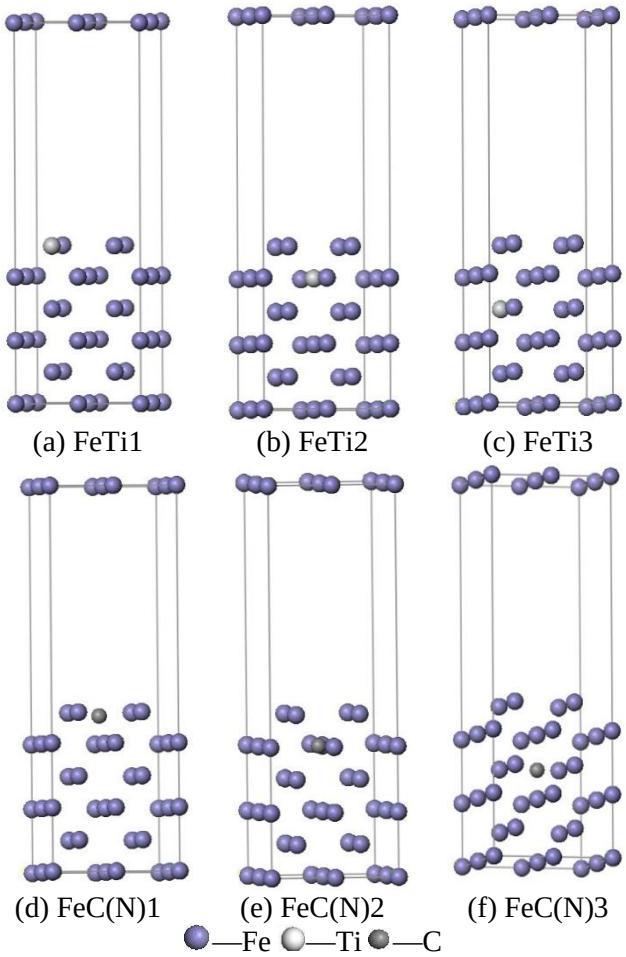

Figure 2. Unit cell model of Ti, C, and N placeholder atoms on each Fe(100) surface layer.

3.2. The binding energy of Fe(100) surfaces with Ti, C, and N

The lattice structure strength and stability strongly relates to the binding energy. The lattice binding energy is the energy released by the formation of free atoms into the lattice structure; in other words, it

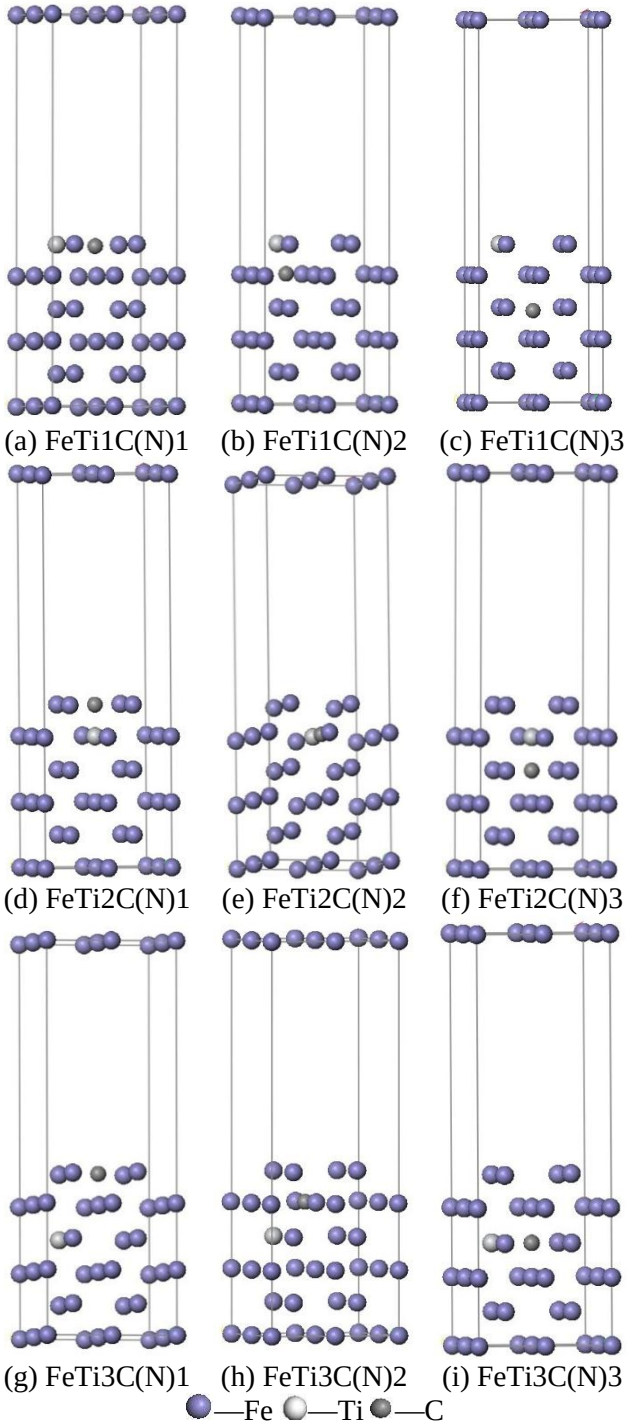

Figure 3. Unit cell model of placeholder Ti and C(N) atoms on the each Fe(100) surface layer.

is the work done by external forces when the lattice decomposes into single atoms. The lower the binding energy (the larger the absolute value), the more stable the lattice will be.

The formula for calculating the binding energy is [15-19]:

$$\Delta E^{ABC} = \frac{1}{N_A + N_B + N_C}\left(E_{tot} - N_A E^A - N_B E^B - N_C E^C\right)$$

In the formula, ΔE^{ABC} is the binding energy, *Etot* is the total energy of the lattice, and E^A, E^B, and E^C are the energies of single atoms A, B, and C respectively. *NA, NB,* and *NC* are the numbers of A, B, and C atoms in the unit cell, respectively. Figures 4-6 show the binding energy of each alloying element shown in the previous figures derived from the above equation.

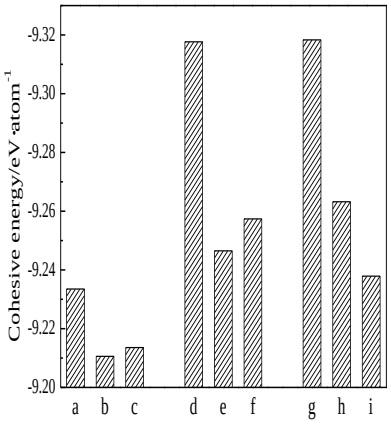

Figure 4. Bonding energy of a Ti, C, and N single atom on an Fe(100) surface.

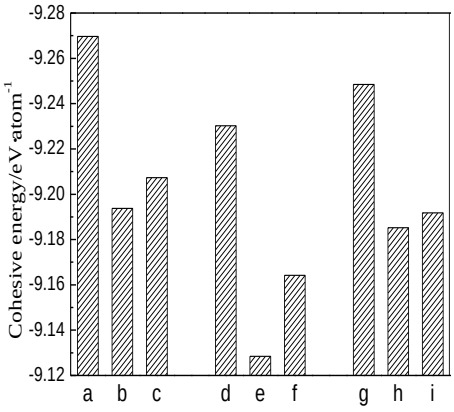

Figure 5. Bonding energy of Ti and C atom placeholders simultaneously on Fe(100) surface.

Figures 4(a)-4(c) represent the binding energy of Ti atoms in the first, second, and third layer of the Fe(100) surface, respectively. d, e, and f represent the binding energy of C atoms in the first, second, and third layer of the Fe(100) surface, respectively. g, h and i represent the binding energy of N atoms in the first, second, and third layer of the Fe(100) surface, respectively.

From figure 4, the binding energies are negative when Fe(100) surface existing single Ti, C, N atoms respectively as solid solution, this means the solid solution could exist stably. When Ti displaces the Fe atoms in the first, third, and second surface layers, the binding energy increases (the absolute value decreases) respectively in order, at the same time the stability decreases gradually. When C is present in the octahedral interstices of the surface first, third, and second layers, the binding energies increase (the absolute value decreases) and stability decreases respectively in order. When N is present in octahedral interstices of the first, second, and third surface layers, the binding energies increase (the absolute value decreases) and stability decreases respectively in order. However, since N migrates to the first layer after being optimized in the second layer, N atoms are unstable when the second octahedral layer on the Fe surface is a solid solution. In conclusion, Ti, C, and N atoms are the most stable when they are in a solid solution respectively in the first layer of Fe(100) surface.

Figures 5(a)-5(c), represent the binding energy of C atoms in the first, second, and third layers when Ti is present only in the first layer. d, e, and f represent the binding energy of C atoms in the first, second, and third layers when Ti is present only in the second layer. g, h, and i represent the binding energy of C atoms in the first, second, and third layers when Ti is present only in the third layer.

From figure 5, when the Fe(100) surface is alloyed by Ti and C, the binding energy is negative, indicating that the both status could exist stably. As can be seen from figures 5(a)-(c), when Ti displaces first layer Fe atoms, the binding energy is the smallest (the absolute value is the biggest) when C is present in the first layer octahedral interstices; this produces the most stable state. The same applies for d, e, and f in figure 5, and for g, h, and i in figure 5 when Ti displaces the second and third layer Fe atoms. Comparing the lowest binding energy of the above mentioned statues shown in figures 5(a), 5(d) and 5(g), the following conclusion can be reached: The binding energy is smallest (the absolute value is biggest) and shows the most stability when Ti displaces the first layer of Fe atoms and C is present in the first layer octahedral interstices.

Figures 6(a)-6(c) respectively represent the binding energy of N atoms in the first, second, and

third layers when Ti is present only in the first layer. d, e, and f respectively represent the binding energy of N atoms in the first, second, and third layers when Ti is present only in the second layer. g, h, and I respectively represent the binding energy of N atoms in the first, second, and third layers when Ti is present only in the third layer.

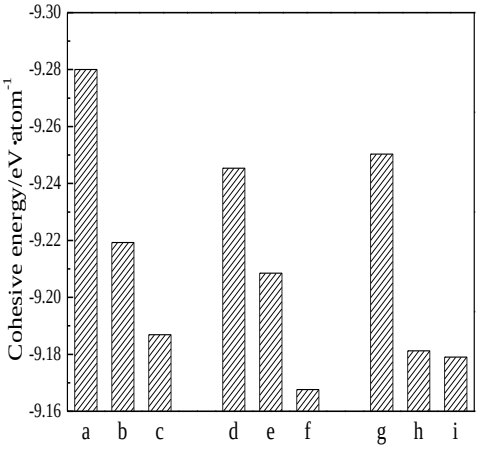

Figure 6. Bonding energy of Ti and N atom placeholder simultaneously on an Fe(100) surface.

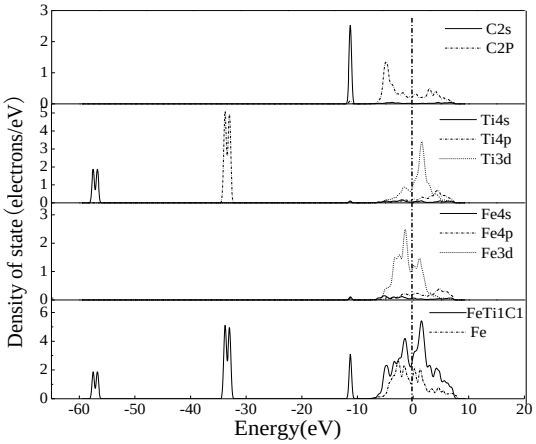

Figure 7. Alloy state densities.

From figure 6, when Fe(100) surface taking place Ti and N alloying, the binding energy is negative, indicating that the both status could stably exist. As can be seen from a, b, and c in figure 6, when Ti displaces the first layer Fe atoms, the binding energy is the smallest (the absolute value is the biggest) when N is present in the first layer octahedral interstices; this produces the most stable state. The same applies when Ti displaces the second (from figures 6(d)-6(f)) and third (from figure 6(g)-6(i)) layer Fe atoms. Comparing the lowest binding energy of the above mentioned statues shown in figures 6(a), 6(d) and 6(g), the following conclusion can be reached: The binding energy is smallest (the absolute value is biggest) and shows the most stability when Ti displaces the first layer of Fe atoms and N is present in the first layer octahedral interstices.

3.3. The density of α-Fe(100) surface states including Ti, C, and N atoms

To a more particular knowledge of the interactions of Ti, C, and N on an Fe(100) surface, the density of states of FeTi1C1and undoped Fe(100) was respectively calculated and shown in figure 7. This shows that the bonding electrons of FeTi1C1 were mainly distributed in the four sections, such as -58.4~ -55.8 eV, -34.8~ -32.0 eV, -12.3~ -10.3 eV, and -8.7~ 8.2 eV. The reactions between Ti, C, N, and Fe atoms were mainly shown as the inter-hybridization between Ti3d, C2p, N2p, and Fe3d orbits near the Fermi level. Also, at a lower Fermi level, the bonding peaks of FeTi1C1 are more two than the peaks without Fe doped. FeTi1C1 has a relatively large pseudogap and its wave is at the Fermi level; Femi levels are closer to the wave crest in Fe state density. This shows that when Ti and C atoms are a solid solution in Fe(100) at the same time, a large amount of covalent and metallic bonds form; without Fe doping, the majority are metallic bonds and only a small amount of covalent bonds are present [20, 21].

In conclusion, the placeholder of Ti, C, and N elements on an Fe(100) surface allow the surface to be hybridized at the electron orbit in the Fermi level, causing the electron bonding peak to increase; this enhances the material's strength and creates stronger pseudogaps near the Fermi level. This shows that Ti, C, and N form solid solutions of the Fe substrate where metallic and covalent bonds could coexist.

4. Conclusion

When single Ti, C, or N atoms occupy positions near the Fe(100) surface, the displacement of Ti atoms with the first layer Fe atoms will result in the best stability. When C or N atoms are present in the octahedral interstice in the first layer on the surface, the stability is at its best. When the Ti and C atoms are accommodated at the same time to the Fe(100) surface, it exhibits the best stability when Ti and C atoms occupy the first layer together. When Ti and N atoms are accommodated to an Fe(100) surface at the same time, it exhibits the best stability when they both occupy the first layer.

After Ti, C, and N form solid solutions on the surface of Fe(100), the orbit electrons of Fe3d, Ti3d, C2p, and N2p will hybridize at Fermi energy, causing the electron bonding peak to increase; this strengthens the binding energy and creates pseudogaps near the Fermi level. That is to say, surface alloying of Ti, C, and N on the Fe substrate will produce covalent bonds, and the metallic bonds will be able to coexist with the covalent bonds.

References

[1] Liu Y P, Xu J Y, Kui X Y, Wang J Z, Gao Y and Xu Z 2005 Study on Microstructure and performance of TiN Multi-permeating Coatings by glow discharge plasma *Transactions of Materials and Heat Treatment* **26** 109-12
[2] Kui X Y,Wang J Z, Liu Y P, Xu J Y, Gao Y and Xu Z 2006 Microstructure and corrosion resistance of TiN coating synthesized by plasma discharge on carbon steel *Corrosion Science and Protection Technology* **18** 12-5
[3] Liu Y P, Xing F and Guo H X 2007 Study on corrosion and wear resistance of ceramic multi-permeating coatings by plasma discharge technique *China Surface Engineering* **20** 19-26
[4] Gao Y, Wang C L, Liu Y P and Xu J Y 2011 Corrosion resistance of TiN layer prepared by double glow plasma surface alloying process *Transactions of Materials and Heat Treatment* **32** 143-7
[5] Liu Y P, Xue J X and Han P D 2010 Electrochemical corrosion behaviors using double glow forming TiN multi-permeation layer *Materials Science Forum* **654** 1968-71
[6] Liu Y P, Xu J Y, Gao Y and Xu Z 2005 A study on TiN/Ti multi-permeations alloying coatings by glow discharge plasma *Materials Review* **19** 112-4
[7] Liu Y P, Xu J Y, Kui X Y and Xu Z 2005 Ceramic alloying with Ti-N deposition and diffusion of multi-layers by plasma surface alloying technique *Trans. Nonferrous Met. Soc. China* **15** 415-9
[8] Zhu Y A, Dai Y C, Chen D and Yuan W K 2007 First-principles study of carbon diffusion in bulk nickel during the growth of fishbone-type carbon nanofibers *Carbon* **45** 21-7
[9] Sorescu D C 2005 First principles calculations of the adsorption and diffusion of hydrogen on Fe(100) surface and in the bulk *Catalysis Today* **105** 44-65
[10] Liu L F, Zhou S Q, Huang Y T and Zhou A R 2008 Computation of diffusion activation energies of C, N and O in α-Fe *Materials Review* **22** 120-2
[11] Segall M D, Lindan P J D, Prober M J, Pickard C J, Hasnip P J, Clark S J and Payne M C 2002 First-principles simulation: Ideas, illustrations and the CASTEP code *J. Phys.: Condens. Matter* **14** 2717-44
[12] Chamati H, Papanicolaou N I and Mishin Y 2006 Embedded-atom potential for Fe and its application to self-diffusion on Fe(100) *Surface Science* **600** 1793-804
[13] Wang X T 1987 *Metal Material Science* (Beijing: Machine industry Press) p 8
[14] Tao M L and Tan X C 2009 Study on first-principles of carbon absorption on Fe(100) surface *Journal of Atomic and Molecular Physics* **26** 349-56
[15] Sorescu D C, Thompson D L, Hurley M M and Chabalowsk C F 2002 First-principles calculations of the adsorption, diffusion, and dissociation of a CO molecule on the Fe(100) surface *Phys. Rev. B* **66** 035416
[16] Zhou D W, Peng P, Hu Y J and Liu J S 2006 Study on structural stability of Mg-Ce intermetallic compounds based on the pseudopotential plane-wave method *Rare Metal Materials and Engineering* **35** 871-5

[17] Zhang C L, Li J M, Han P D, Chi M, Yan L Y, Liu X G and Xu B S 2008 Study on alloying effects of Ni3Al with Cr based on the pseudopotential plane-wave method *Rare Metal Materials and Engineering* **37** 1705-9
[18] Huang Z W, Zhao Y H, Hou H, Wang Z, Mu Y Q, Niu X F and Han P D 2011 Point defects structure and alloying effects of V atoms into Ni3Al alloy: A first-principles study *Rare Metal Materials and Engineering* **12** 2136-41
[19] Zhao Y H, Huang Z W, Li A H, Mu Y Q, Yang M H, Hou H, Han P D and Zhang S Y 2011 First principles study on substitution behavior and alloying effects of Nb in Ni_3Al *Acta Phys. Sin.* **60** 047103-49
[20] Chen Y, Shang J X and Zhang Y 2007 Effects of alloying element Ti on α-Nb5Si3 and Nb3Al from first principles *Phys: Condens Matter* **19** 016215
[21] Hu M Q, Yang R, Xu D S, Hao Y L and Li D 2003 Geometric and electronic structure of Ti_2AlX(X=V, Nb, or Ta) *Phys. Rev. B* **68** 054102